International Journal of Applied Mechanics
Vol. 4, No. 1 (2012) 1250003 (12 pages)

DOI: 10.1142/S1758825112001324

Imperial College Press
www.icpress.co.uk

PULL-IN INSTABILITY OF CIRCULAR PLATE MEMS: A NEW MODEL BASED ON STRAIN GRADIENT ELASTICITY THEORY

BINGLEI WANG[*,†], SHENJIE ZHOU[†,¶]
JUNFENG ZHAO[*,†] and XI CHEN[†,‡,§,‖]

[*]*School of Civil Engineering*
Shandong University, Jinan City, Shandong 250061, China

[†]*School of Mechanical Engineering*
Shandong University, Jinan City, Shandong 250061, China

[‡]*School of Aerospace, Xi'an Jiaotong University, Xi'an 710049, China*

[§]*Department of Civil and Environmental Engineering*
Hanyang University, Seoul, 133-791, Korea

[¶]*zhousj@sdu.edu.cn*
[‖]*xichen@columbia.edu*

Received 19 January 2011
Accepted 11 April 2011
Published 31 March 2012

Size-dependent characteristics have been widely observed in microscale devices. For the electrostatically actuated circular microplate-based MEMS, we propose a new model to predict the size-dependent pull-in instability based on the strain gradient elasticity theory. The model embeds three material length scale parameters (MLSPs), which can effectively predict the size-dependent pull-in voltage. The model can be reduced to the classical continuum model when MLSPs are ignored. The results show that the normalized pull-in voltage predicted by the present model increases nonlinearly with the decrease of the size scale of the plate, and the size effect becomes prominent if the characteristic dimension (plate thickness) is on the order of microns or smaller. The effects of the plate thickness and gap on the pull-in voltage are also investigated.

Keywords: Size effect; strain gradient elasticity; circular microplate; pull-in voltage.

1. Introduction

MEMS-based electrostatic devices are essentially simple capacitors composed of two parallel microplates, usually with a square, circular or beam-type configuration. One of the two microplates is fixed and the other is deformable as shown in Fig. 1. Under an applied voltage, the upper movable electrode deflects towards the fixed electrode due to electrostatic attraction. As the voltage increases beyond a critical value, the movable electrode becomes unstable and collapses onto the fixed electrode. The critical displacement and the critical voltage associated with this instability

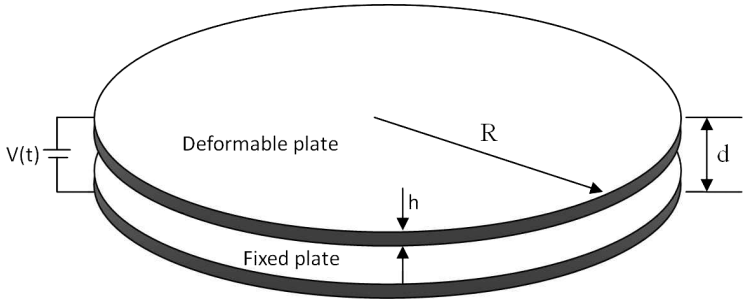

Fig. 1. Schematic of electrostatically actuated circular microplate-based MEMS (the edge of the upper plate is fixed).

are referred to as the pull-in displacement and the pull-in voltage, respectively. In microresonators (e.g., microphones and microsensors) the designer should avoid such instability in order to achieve stable motions; however, in switching applications the designer takes advantage of this effect to optimize the performance of the device.

Among various types of MEMS devices, the circular-plate-based ones yield better structural reliability than rectangular plates, since the corner and/or sharp edges in rectangular plates may induce high residual stress after multiple depositions [Liao *et al.*, 2010]. An analytical reduced-order model (macromodel) for an electrically actuated clamped circular plate was presented by Vogl and Nayfeh [2005], which accounts for both residual stress and strain hardening. Batra *et al.* [2008] developed a different macromodel (where the bending stiffness was neglected and the plate was taken to be a membrane) to study the effect of the Casimir force. Liao *et al.* [2010] developed a continuum model to analyze the "pull-in" effect in the circular microplate, where only first-order deflection mode was considered and closed-form solutions were obtained for both the position and voltage of the static pull-in event. Bertarelli *et al.* [2011] studied the mechanical response of circular microplates undergoing electrostatic actuation. A one degree-of-freedom model and Finite Element approaches were exploited in a nondimensional framework.

All previous models were based on conventional elasticity and there was no size effect. When the size of the device continues to decrease, the size-dependent behavior has been experimentally observed in microstructures made of metal [Fleck *et al.*, 1994; Poole *et al.*, 1996], polymer [Lam and Chong, 1999; Lam *et al.*, 2003; McFarland and Colton, 2005] and polysilicon [Aifantis, 2009; Chasiotis and Knauss, 2003]. For example, Chasiotis and Knauss [2003] observed that the failure stress at the tip of a perforated MEMS polycrystalline silicon exhibits strong size effect: The nominal average failure stress increased nonlinearly as the hole radius was decreased from 16 μm to 1 μm, however according to the classical mechanics theory, the nominal average failure stress should be a constant; this size-dependent behavior was successfully simulated using the gradient elastic theory by Aifantis [2009].

Various higher-order microscale theories have been developed since 1960s. Some of them were applied to study the microscale circular plate, including the micropolar theory [Ariman, 1968], the gradient elastic theory [Duan *et al.*, 2007], and the nonlocal theory [Papargyri-Beskou *et al.*, 2010]. These theories, however, either contain too many variables (thus not convenient) or do not have explicit physical background. Comparing with other higher-order microscale continuum theories (where often only one material length scale parameter (MLSP) is included), the strain gradient elasticity theory proposed by Lam *et al.* [2003] contains three material length scale parameters which correspond to the dilatation gradient tensor, the deviatoric stretch gradient tensor, and the symmetric rotation gradient tensor, so as to take full advantage of the higher-order items. The theory has been used to analyze the static and dynamic behaviors of the microscale Bernoulli–Euler beam [Kong *et al.*, 2009] and Timoshenko beam [Wang *et al.*, 2010]. Nevertheless, the mechanical–electrical coupled properties of the microscale axisymmetric circular plate have not yet been studied to the best of our knowledge.

The paper aims to fill this gap by developing a size-dependent mechanical–electrical coupled circular plate model based on strain gradient elasticity, and as an illustration for evaluating the mechanical integrity of MEMS; the model is employed to study the pull-in instability of electrostatically actuated circular microplate-based device.

2. The Size-Dependent Model

Figure 1 shows a typical circular-plate-based electrostatically actuated device, which consists of a fixed electrode and a deformable microplate with density ρ, radius R and thickness h, separated by a dielectric spacer with an initial gap d. With an applied voltage V, the upper plate deflects towards the fixed electrode under the combined action of the distributed electrostatic load Fe and elastic restoring force. At a critical pull-in voltage, the microplate loses its stability and spontaneously collapses onto the fixed electrode.

The strain gradient elasticity theory, proposed by Lam *et al.* [2003], can predict the size effect of micron and submicron devices. Three independent MLSPs are introduced to characterize the size effect. The strain energy U in a deformed isotropic linear elastic material occupying region ψ (with a volume element Ω) is given by

$$U = \frac{1}{2}\int_{\psi}(\sigma_{ij}\varepsilon_{ij} + p_i\gamma_i + \tau^{(1)}_{ijk}\eta^{(1)}_{ijk} + m^s_{ij}\chi^s_{ij})d\Omega, \tag{1}$$

where the strain tensor, ε_{ij}, the dilatation gradient tensor, γ_i, the deviatoric stretch gradient tensor, $\eta^{(1)}_{ijk}$, and the symmetric rotation gradient tensor, χ^s_{ij}, are defined by

$$\varepsilon_{ij} = \frac{1}{2}(\partial_j u_i + \partial_i u_j), \tag{2}$$

$$\eta_{ijk}^{(1)} = \eta_{ijk}^{s} - \frac{1}{5}(\delta_{ij}\eta_{mmk}^{s} + \delta_{jk}\eta_{mmi}^{s} + \delta_{ki}\eta_{mmj}^{s}), \tag{3}$$

$$\gamma_i = \partial_i \varepsilon_{mm}, \tag{4}$$

$$\chi_{ij}^{s} = \frac{1}{4}(e_{ipq}\partial_p \varepsilon_{qj} + e_{jpq}\partial_p \varepsilon_{qi}), \tag{5}$$

respectively. Here, ∂_i is the differential operator, u_i is the displacement vector, ε_{mm} is the dilatation strain, and η_{ijk}^{s} is the symmetric part of the second-order displacement gradient tensor:

$$\eta_{ijk}^{s} = \frac{1}{3}(u_{i,jk} + u_{j,ki} + u_{k,ij}), \tag{6}$$

where δ_{ij} and e_{ijk} are the Kronecker delta and permutation tensor, respectively. The stress measures include the classical stress tensor, σ_{ij}, and the higher-order stresses, p_i, $\tau_{ijk}^{(1)}$, and m_{ij}^{s}, which are the work-conjugate to the deformation measures, are given by the following:

$$\sigma_{ij} = k\delta_{ij}\varepsilon_{mm} + 2\mu\varepsilon'_{ij}, \tag{7}$$

$$p_i = 2\mu l_0^2 \gamma_i, \tag{8}$$

$$\tau_{ijk}^{(1)} = 2\mu l_1^2 \eta_{ijk}^{(1)}, \tag{9}$$

$$m_{ij}^{s} = 2\mu l_2^2 \chi_{ij}^{s}, \tag{10}$$

where $\varepsilon'_{ij} = \varepsilon_{ij} - \frac{1}{3}\varepsilon_{mm}\delta_{ij}$ is the deviatoric strain. k and μ are the bulk and shear modulus, respectively. l_0, l_1 and l_2 are the independent MLSPs associated with γ_i, $\eta_{ijk}^{(1)}$, and χ_{ij}^{s}, respectively.

Wang *et al.* [2011a] proposed a size-dependent model for a rectangular Kirchhoff plate based on the strain gradient elasticity theory. For a microplate with external force $q(x, y)$ applied, the governing equation is:

$$-p_1\bar{\nabla}^6 w + p_2\bar{\nabla}^4 w + \frac{\partial^2 w}{\partial t^2} = q(x, y), \tag{11}$$

in which:

$$\begin{aligned} p_1 &= I\mu\left(2l_0^2 + \frac{4}{5}l_1^2\right), \\ p_2 &= \mu h\left(2l_0^2 + \frac{8}{15}l_1^2 + l_2^2\right) + \left(k + \frac{4}{3}\mu\right)I \end{aligned} \tag{12}$$

and

$$\begin{aligned} \bar{\nabla}^6 w &= \frac{\partial^6 w}{\partial x^6} + 3\frac{\partial^6 w}{\partial x^4 \partial y^2} + 3\frac{\partial^6 w}{\partial x^2 \partial y^4} + \frac{\partial^6 w}{\partial y^6}, \\ \bar{\nabla}^4 w &= \frac{\partial^4 w}{\partial x^4} + 2\frac{\partial^4 w}{\partial x^2 \partial y^2} + \frac{\partial^4 w}{\partial y^4}. \end{aligned} \tag{13}$$

$I = h^3/12$ is the moment of inertia, t is time.

However, the governing equation above is expressed in the Cartesian coordinate system. For application in circular microplate, they must be transformed to the cylindrical coordinate system. The electric force works as the external force $q(x, y)$, which is expressed as:

$$q(x, y) = \frac{\varepsilon V^2}{2(d-w)^2}, \tag{14}$$

in which ε is the dielectric constant of the gap medium.

Dimensionless variables ($\bar{w} = \frac{w}{d}; \bar{r} = \frac{r}{R}; \bar{t} = \frac{t}{T}$, T is a time scale defined below) are substituted to the governing equation in cylindrical coordinate systems and after removing all the hats of the variables. The dimensionless governing equations become:

$$\alpha_1 \nabla^6 w + \nabla^4 w + \frac{\partial^2 w}{\partial t^2} = \frac{\alpha_2 V^2}{(1-w)^2}, \tag{15}$$

where

$$\begin{aligned}\nabla^6 &= \left(\frac{\partial^2}{\partial r^2} + \frac{1}{r}\frac{\partial}{\partial r}\right)\left(\frac{\partial^2}{\partial r^2} + \frac{1}{r}\frac{\partial}{\partial r}\right)\left(\frac{\partial^2}{\partial r^2} + \frac{1}{r}\frac{\partial}{\partial r}\right)\\ &= \frac{\partial^6}{\partial r^6} + \frac{3}{r}\frac{\partial^5}{\partial r^5} + \frac{3}{r^2}\frac{\partial^4}{\partial r^4} + \frac{1}{r^3}\frac{\partial^3}{\partial r^3},\end{aligned} \tag{16}$$

$$\nabla^4 = \left(\frac{\partial^2}{\partial r^2} + \frac{1}{r}\frac{\partial}{\partial r}\right)\left(\frac{\partial^2}{\partial r^2} + \frac{1}{r}\frac{\partial}{\partial r}\right) = \frac{\partial^4}{\partial r^4} + \frac{2}{r}\frac{\partial^3}{\partial r^3} + \frac{1}{r^2}\frac{\partial^2}{\partial r^2},$$

$$\alpha_1 = \frac{S}{R^2 D'}, \quad \alpha_2 = \frac{R^4 \varepsilon}{2D' d^3}, \quad T^2 = \frac{\rho h R^4}{D'}, \tag{17}$$

and

$$\begin{aligned} S &= -I\mu\left(2l_0^2 + \frac{4}{5}l_1^2\right)\\ D' &= \mu h\left(2l_0^2 + \frac{8}{15}l_1^2 + l_2^2\right) + \left(k + \frac{4}{3}\mu\right)I.\end{aligned} \tag{18}$$

The classical boundary conditions for the dimensionless axisymmetric circular plate are

$$\begin{aligned} w = 0; \quad \frac{dw}{dr} = 0 \quad \text{at } r = 1,\\ \frac{dw}{dr} = 0; \quad \frac{d^3 w}{dr^3} + \frac{1}{r}\frac{d^2 w}{dr^2} - \frac{1}{r^2}\frac{dw}{dr} = 0; \quad \text{at } r = 0.\end{aligned} \tag{19}$$

Note that different forms of higher order boundary conditions have almost no effect on the final results [Kong *et al.*, 2009]. For simplicity, following Papargyri-Beskou and Beskos [2008], we assume a very simple form for the higher-order boundary condition as

$$\frac{\partial^4 w}{\partial r^4} = 0; \quad \text{at } r = 0, 1. \tag{20}$$

In conclusion, all the boundary conditions employed in the present study are:

$$\begin{gathered} w = 0; \quad \frac{dw}{dr} = 0; \quad \frac{d^4 w}{dr^4} = 0 \quad \text{at } r = 1, \\ \frac{dw}{dr} = 0; \quad \frac{d^3 w}{dr^3} + \frac{1}{r}\frac{d^2 w}{dr^2} - \frac{1}{r^2}\frac{dw}{dr} = 0; \quad \frac{d^4 w}{dr^4} = 0 \quad \text{at } r = 0. \end{gathered} \tag{21}$$

It is noted that when the MLSPs are ignored (i.e., $l_0 = l_1 = l_2 = 0$), the sixth-order term in the governing equation (15) vanishes; in that case, the present model with size effect can be reduced to the classical model without size effect [Liao *et al.*, 2010; Vogl and Nayfeh, 2005].

3. Application of GDQ Method

The GDQ method is adopted in this paper to solve the governing equation (15) combining with the boundary conditions Eq. (21). This method is based on the idea that the derivative of a function with respect to a coordinate can be expressed as a weighted linear summation of function values at all mesh points along that direction. Consider a function $w(r)$which is defined in the domain $0 \le r \le 1$. The mth-order derivative of the function $w(r)$ at the ith point, r_i in radial direction is approximated as (where r_i is the Chebyshev–Gauss–Lobatto node):

$$\frac{\partial^m w(r_i)}{\partial r^m} = \sum_{j=1}^{N} c_{ij}^{(m)} w(r_i), \quad i = 1, 2, \ldots, N, \tag{22}$$

where $c_{ij}^{(m)}$ is a weighting factor. $c_{ij}^{(1)}$ $(i, j = 1, 2, \ldots, N)$ is expressed as

$$\begin{gathered} c_{ij}^{(1)} = M^{(1)}(r_i)/(r_i - r_j)M^{(1)}(r_j) \quad \text{for } i \neq j, \quad i = 1, 2, \ldots, N, \\ c_{ii}^{(1)} = -\sum_{\substack{j=1 \\ j \neq i}}^{N} c_{ij}^{(1)} \quad \text{for } i = 1, 2, \ldots, N, \end{gathered} \tag{23}$$

where

$$M^{(1)}(r_j) = \prod_{k=1, k \neq j}^{N} (r_j - r_k). \tag{24}$$

The weighting coefficients for higher-order derivatives can be obtained as:

$$\begin{gathered} c_{ij}^{(m)} = m\left(c_{ii}^{(m-1)} c_{ij}^{(1)} - \frac{c_{ij}^{(m-1)}}{r_i - r_j}\right) \quad \text{for } i \neq j, \quad m = 2, 3, \ldots, N-1, \\ i, j = 1, 2, \ldots, N, \\ c_{ii}^{(m)} = -\sum_{j=1, j \neq i}^{N} c_{ij}^{(m)} \quad \text{for } i = 1, 2, \ldots, N. \end{gathered} \tag{25}$$

By applying the GDQ method, Eq. (15) is rewritten in tensor form:

$$\boldsymbol{\alpha}_1\left(\mathbf{C^{(6)}}+\frac{3}{\mathbf{R}}\mathbf{C^{(5)}}+\frac{3}{\mathbf{R^2}}\mathbf{C^{(4)}}+\frac{1}{\mathbf{R^3}}\mathbf{C^{(3)}}\right)\mathbf{W}$$
$$+\left(\mathbf{C^{(4)}}+\frac{2}{\mathbf{R}}\mathbf{C^{(3)}}+\frac{1}{\mathbf{R}^2}\mathbf{C^{(2)}}\right)\mathbf{W}=\alpha_2\widehat{\mathbf{V}},\quad \mathbf{W}=(w_1,w_2,\ldots,w_N)^T, \tag{26}$$

where

$$\widehat{\mathbf{V}}=\left(\frac{V^2}{(1-w_1)^2},\frac{V^2}{(1-w_2)^2},\ldots,\frac{V^2}{(1-w_N)^2}\right)^T, \tag{27}$$

$$\mathbf{C}^{(k)}=\begin{bmatrix} c_{11}^{(k)} & c_{12}^{(k)} & \cdots & c_{1N}^{(k)}\\ c_{21}^{(k)} & c_{22}^{(k)} & \cdots & c_{2N}^{(k)}\\ \vdots & \vdots & \ddots & \vdots\\ c_{N1}^{(k)} & c_{N2}^{(k)} & \cdots & c_{NN}^{(k)}\end{bmatrix}\quad\text{and}\quad \mathbf{R}=\begin{bmatrix} r_1 & 0 & \cdots & 0\\ 0 & r_2 & \cdots & 0\\ \vdots & \vdots & \ddots & \vdots\\ 0 & 0 & \cdots & r_N\end{bmatrix}. \tag{28}$$

The boundary conditions (21) are rewritten as

$$\begin{gathered} w_N=0;\quad \sum_{j=1}^{N}e_{Nj}^{(1)}w_j=0;\quad \sum_{j=1}^{N}e_{Nj}^{(4)}w_j=0;\quad \sum_{j=1}^{N}e_{1j}^{(1)}w_j=0,\\ \sum_{j=1}^{N}e_{1j}^{(3)}w_j+\sum_{j=1}^{N}\frac{1}{r_j}e_{1j}^{(2)}w_j-\sum_{j=1}^{N}\frac{1}{r_j^2}e_{1j}^{(1)}w_j=0;\quad \sum_{j=1}^{N}e_{1j}^{(4)}w_j=0. \end{gathered} \tag{29}$$

Solving the discrete governing equation (26) combining with the discrete boundary condition Eq. (29), the bending displacement $w(r)$ can be numerically determined.

4. Results and Discussion

With the three MLSPs involved, the present model can predict the size-dependent properties for electrostatically actuated circular microplate-based devices. It should be noted that the MLSPs are internal parameters of a given material, which can be obtained from uniaxial tensile or bending experiments. For simplicity, it is assumed that the three constants are the same and equal to Cl throughout the following discussion, i.e., $l_0=l_1=l_2=Cl$. For the rest of this paper, the Young's Modulus of the plate is $E=151\,\text{GPa}$ and Poisson's ratio $\nu=0.3$.

When applying the GDQ method in the numerical procedure, the number of discrete points (nodes) in the radial direction is chosen as $N=21$, which is proven to be accurate for this problem [Kuang and Chen, 2004]. Convergence, with a tolerance of 10^{-8}, can be achieved within four iterations with the help of the pseudo arc-length algorithm [Klosiewicz *et al.*, 2009; Nayfeh and Balachandran, 1995].

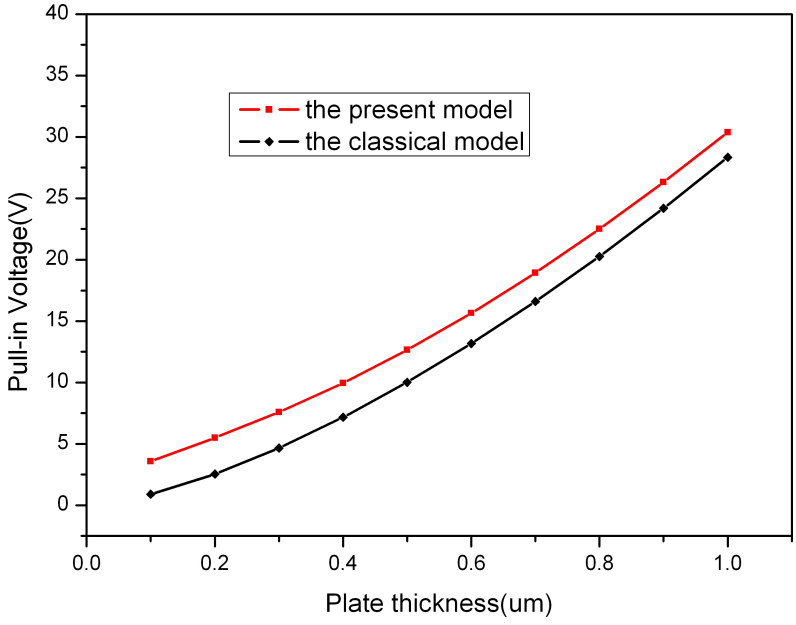

Fig. 2. Pull-in voltage variation with plate thickness.

First, to illustrate the newly developed model, the pull-in voltage predicted by the present model is studied with the variation of plate thickness (h, from 0.1 μm to 1.0 μm) as depicted in Fig. 2. The parameters used in this example are $R = 200\mu$m and $g = 0.5\,\mu$m, Cl is taken to be 0.1 μm. For comparison, the corresponding results predicted by the classical model (without size effect) are also shown. For both models, the pull-in voltage increases as the plate gets thicker, indicate that a thicker plate needs larger voltage to deform the upper plate, owing to the higher bending rigidity. Meanwhile, the present model predicts larger pull-in voltage than the classical model, since the three additional gradient tensors result in higher rigidity than the classical model, which is consistent with literature [Kong *et al.*, 2009; Wang *et al.*, 2010, 2011b]. The result of the present model is 3.97 times of the classical model when $h = 0.1\,\mu$m, yet the ratio decreases to 1.07 when $h = 1.0\,\mu$m, indicating a strong size effect which will be discussed below.

Next, we study the variation of the pull-in voltage with plate gap (g, from 0.1μm to 1.0 μm) in Fig. 3. In this case, $R = 200\,\mu$m and $h = 0.5\,\mu$m, Cl is still taken to be 0.1 μm. The pull-in voltage is found to increase as the gap gets larger (due to the required larger deformation). Although the results predicted by the present model are higher than those by the classical model, the difference between the two models is small when gap $g = 0.1\,\mu$m, yet the difference increases for larger gap, also exhibiting a strong size effect.

Finally, to further demonstrate the size effect, a size scale k is defined as the ratio of plate thickness to MLSP, i.e., $k = h/Cl$; in Fig. 4 we plot the normalized

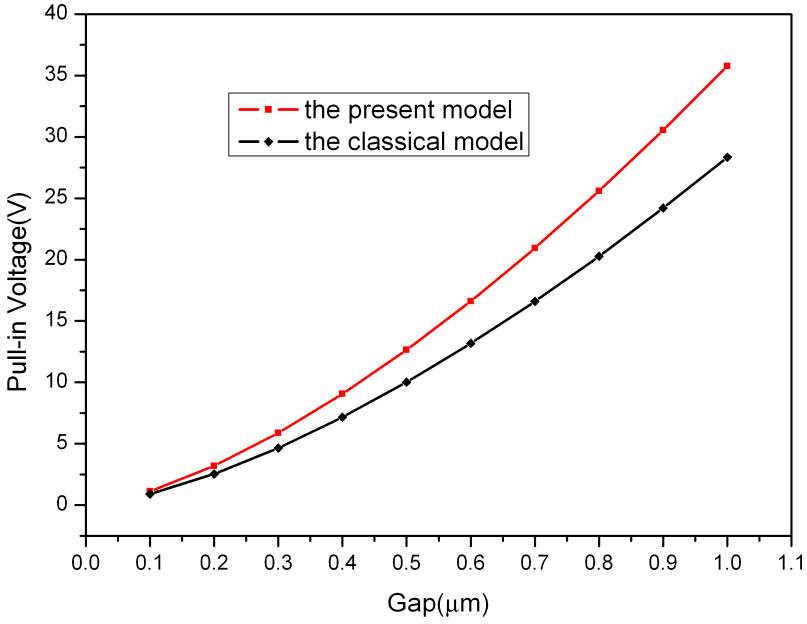

Fig. 3. The pull-in voltage versus gap.

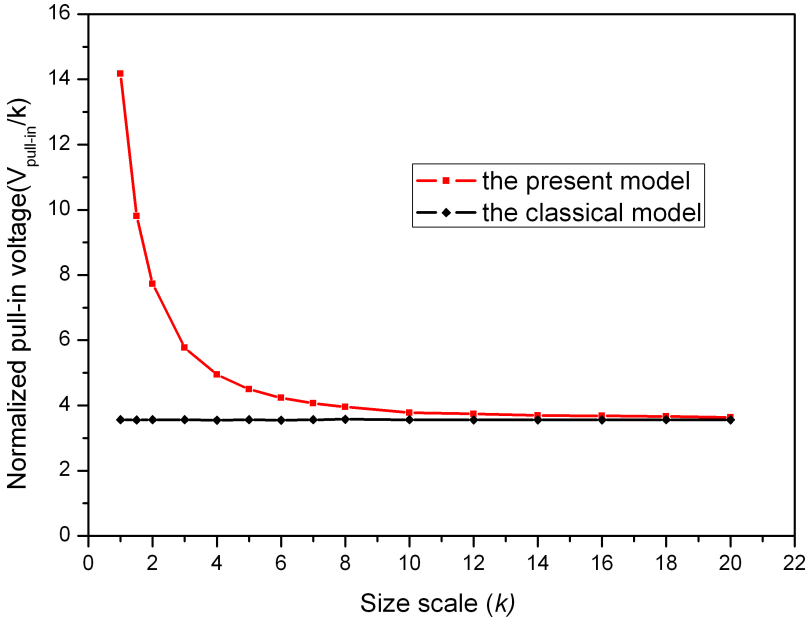

Fig. 4. The normalized pull-in voltage varies with size scale.

pull-in voltage ($V_{\text{pull}-\text{in}}/k$) with respect to k. Here, we keep the plate shape to be the same, i.e., fixing $R/h = 300$ and the gap between the movable plate and fixed electrode is kept as $g/h = 1$. Since Cl is still taken to be $0.1\,\mu$m, the variation of the size scale k indicates different device sizes (while the plate's shape is fixed). For the present model, the normalized pull-in voltage $V_{\text{pull-in}}/k$ increases nonlinearly as the size scale k decreases, or when the MLSP becomes more prominent comparing with the plate characteristic dimension (i.e., the thickness h), showing strong size-dependence. However, for the classical model, the normalized pull-in voltage keeps a constant despite the variation of the size scale. Moreover, the two models show almost no difference for the normalized pull-in voltage if k is about larger than 15, indicating that the present model can also be applied at the macro scale; in other words, the size effect is diminishing if the plate thickness is more than 15 times the MLSP (i.e., if the plate thickness is several microns or larger). The strong size effect indicates that the classical model may be inadequate at submicron scale. Specifically, when the size scale $k = 1$ and 6, the normalized pull-in voltage predicted by the present model are 3.97 and 1.19 times of that by the classical model, respectively. The similar tendency was discovered by Lam *et al.* [2003], where in their experiment, the normalized bending rigidity was increased by 2.4 times when the beam thickness was reduced from 115 to $20\,\mu$m, and that was successfully predicted by using the strain gradient elasticity theory with MLSP included.

5. Conclusion

Based on the strain gradient elasticity theory, a size-dependent model for electrostatically actuated circular microplate-based MEMS device is established. The size-dependent pull-in voltage is studied by solving the higher-order governing equation numerically. The influence of the plate thickness and plate gap on the pull-in voltage is investigated. Furthermore, the normalized pull-in voltage with size scale is also explored. The results show that the normalized pull-in voltage keeps a constant for the classical model, while it increases nonlinearly with decreasing size scale for the present model. Such a size effect is especially strong when the size scale is smaller than about 15. Therefore, the newly developed model is in particular useful at submicron scales. Meanwhile, the size effect diminishes if the plate thickness is several microns or more (at least 15 times MLSP), or if the strain gradient effect is ignored. The new model may be robust for describing the behavior of size-dependent pull-in instability for circular microplate-based MEMS devices, at both micro- and macro-scales.

Acknowledgments

The work is supported by Independent Innovation Fund of Shandong University (2011GN055). XC acknowledges support from National Science Foundation (CMMI-0643726), DARPA (W91CRB-11-C-0112), Changjiang Scholar Program

from Ministry of Education of China, and National Natural Science Foundation of China (11172231 and 50928601).

References

Aifantis, E. C. [2009] "Exploring the applicability of gradient elasticity to certain micro/nano reliability problems," *Microsystem Technologies-Micro-and Nanosystems-Information Storage and Processing Systems* **15**, 109–115.

Ariman, T. [1968] "On circular micropolar plates," *Ingenieur Archiv* **37**, 156–160.

Batra, R. C., Porfiri, M. and Spinello, D. [2008] "Reduced-order models for microelectromechanical rectangular and circular plates incorporating the Casimir force," *International Journal of Solids and Structures* **45**, 3558–3583.

Bertarelli, E., Ardito, R., Corigliano, A. and Contro, R. [2011] "A plate model for the evalualuation of pull-in instability occurrence in electrostatic micropump diaphragms," *International Journal of Applied Mechanics* **3**, 1–19.

Chasiotis, I. and Knauss, W. G. [2003] "The mechanical strength of polysilicon films: Part 2. Size effects associated with elliptical and circular perforations," *Journal of the Mechanics and Physics of Solids* **51**, 1551–1572.

Duan, W. H. and Wang, C. M. [2007] "Exact solutions for axisymmetric bending of micro/nanoscale circular plates based on nonlocal plate theory," *Nanotechnology* **18**, 385704.

Fleck, N. A., Muller, G. M., Ashby, M. F. and Hutchinson, J. W. [1994] "Strain gradient plasticity theory and experiment," *Acta Metallurgica Et Materialia* **42**, 475–487.

Klosiewicz, P., Broeckhove, J. and Vanroose, W. [2009] "Using pseudo-arclength continuation to trace the resonances of the Schrodinger equation," *Computer Physics Communications* **180**, 545–548.

Kong, S. L., Zhou, S. J., Nie, Z. F. and Wang, K. [2009] "Static and dynamic analysis of micro beams based on strain gradient elasticity theory," *International Journal of Engineering Science* **47**, 487–498.

Kuang, J. H. and Chen, C. J. [2004] "Dynamic characteristics of shaped micro-actuators solved using the differential quadrature method," *Journal of Micromechanics and Microengineering* **14**, 647–655.

Lam, D. C. C. and Chong, A. C. M. [1999] "Indentation model and strain gradient plasticity law for glassy polymers," *Journal of Materials Research* **14**, 3784–3788.

Lam, D. C. C., Yang, F., Chong, A. C. M., Wang, J. and Tong, P. [2003] "Experiments and theory in strain gradient elasticity," *Journal of the Mechanics and Physics of Solids* **51**, 1477–1508.

Liao, L. D., Chao, P. C. P., Huang, C. W. and Chiu, C. W. [2010] "dc dynamic and static pull-in predictions and analysis for electrostatically actuated clamped circular microplates based on a continuous model," *Journal of Micromechanics and Microengineering* **20**, 025013 (15 pp).

McFarland, A. W. and Colton, J. S. [2005] "Role of material microstructure in plate stiffness with relevance to microcantilever sensors," *Journal of Micromechanics and Microengineering* **15**, 1060–1067.

Nayfeh, A. H. and Balachandran, B. [1995] *Applied Nonlinear Dynamics* (New York, Wiley).

Papargyri-Beskou, S. and Beskos, D. E. [2008] "Static, stability and dynamic analysis of gradient elastic flexural Kirchhoff plates," *Archive of Applied Mechanics* **78**, 625–635.

Papargyri-Beskou, S., Giannakopoulos, A. E. and Beskos, D. E. [2010] "Variational analysis of gradient elastic flexural plates under static loading," *International Journal of Solids and Structures* **47**, 2755–2766.

Poole, W. J., Ashby, M. F. and Fleck, N. A. [1996] "Micro-hardness of annealed and work-hardened copper polycrystals," *Scripta Materialia* **34**, 559–564.

Vogl, G. W. and Nayfeh, A. H. [2005] "A reduced-order model for electrically actuated clamped circular plates," *Journal of Micromechanics and Microengineering* **15**, 684–690.

Wang, B., Zhao, J. and Zhou, S. [2010] "A microscale Timoshenko beam model based on strain gradient elasticity theory," *European Journal of Mechanics — A/Solids* **29**, 591–599.

Wang, B., Zhao, J., Zhou, S. and Chen, X. [2011a] "A size-dependent kirchhoff micro-plate model based on strain gradient elasticity theory," *European Journal of Mechanics — A/Solids* **30**, 517–524.

Wang, B., Zhao, J., Zhou, S. and Chen, X. [2011b] "Size-dependent pull-in instability of electrostatically actuated microbeam-based MEMS," *Journal of Micromechanics and Microengineering* **21**, 027001.